BARE-GROUND SURFACE HEAT AND WATER EXCHANGES UNDER DRY CONDITIONS: OBSERVATIONS AND PARAMETERIZATION

I. BRAUD, J. NOILHAN, P. BESSEMOULIN, P. MASCART

Météo-France/CNRM, 31057 Toulouse Cédex, France

and

R. HAVERKAMP, M. VAUCLIN

LTHE/IMG, CNRS URA 1512, INPG, UJF BP 53 X, 38041 Grenoble Cédex, France

(Received in final form 12 February, 1993)

Abstract. A simplified land-surface parameterization is tested against bare-soil data collected during the EFEDA experiment conducted in Spain in June 1991. A complete data set, made up of soil properties as well as hydrological and atmospheric measurements, is described and discussed. The 11-day data set is characterized by very dry conditions and high surface temperatures during the day. Large values of sensible and soil heat fluxes and small values of surface evaporation ($\approx$1 mm/day) were observed.

This data set was modelled, leading to the following conclusions:

(i) In the model, the parameterization provides values of the soil thermal properties and subsequently of the predicted soil heat fluxes which are overestimated when compared with the observations.

(ii) Following the literature, a value of the ratio between the roughness lengths for momentum Z_o and heat Z_{oh} of close to 10 for fairly homogeneous areas of bare soil and vegetation is used. This value leads to a fair prediction of the surface temperature. If the roughness lengths were taken to be equal, as is often assumed in atmospheric modelling, a poorer prediction results.

(iii) Finally, the vapor phase transfer mode is found dominant close to the surface and a modified parameterization including this effect is proposed. It allows a fair prediction of both surface evaporation and near-surface water content.

1. Introduction

During the last ten years, significant progress has been made in the parameterization of land-surface processes in atmospheric models, especially thanks to field experiments such as Hapex–Mobilhy (André *et al.*, 1986) or FIFE (Sellers *et al.*, 1988). They provided data sets of the surface mass and energy budgets at the regional scale, which were used to improve and validate land-surface schemes. However, most of these data were collected in a temperate climate. The recent Echival Field Experiment in a Desertification Threatened Area (EFEDA, Bolle *et al.*, 1992) was conducted in a drier climate, in order to test the validity of various surface schemes under extreme soil conditions. The experiment took place in Spain, in the region of Castilla–La Mancha. It was mainly designed to collect the various components of mass and heat exchanges, over a study area of $100 \times 100\,\mathrm{km}^2$, at various time and space scales. The mean altitude of this area is between 600 and 700 m and the area is surrounded by mountains to its north, east

Boundary-Layer Meteorology **66**: 173–200, 1993.
© 1993 *Kluwer Academic Publishers. Printed in the Netherlands.*

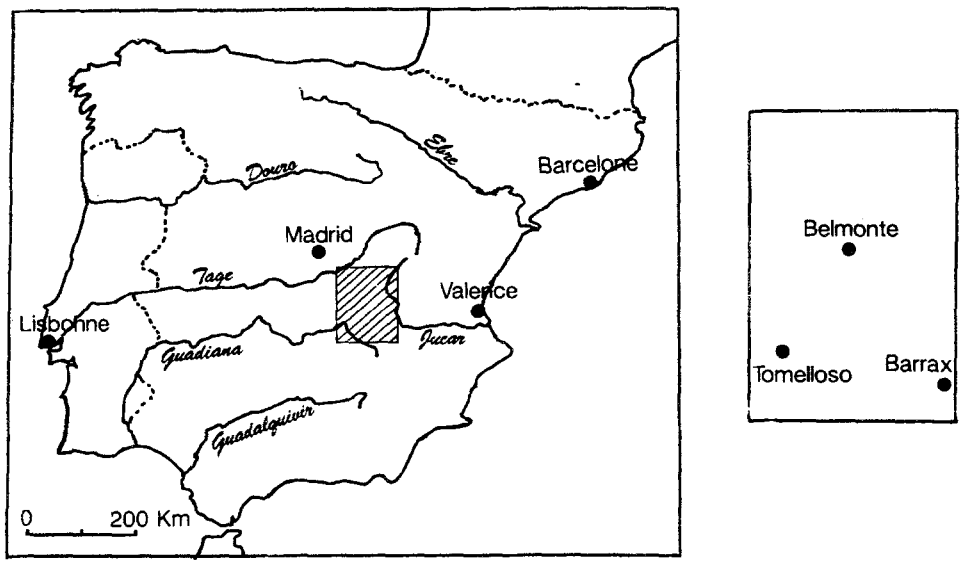

Fig. 1. The study area in Spain with the three sites instrumented during the Intensive Observation Period.

and south. The region has a moderately warm, dry Mediterranean climate, with continental characteristics, especially large diurnal and annual temperature ranges. Three sites were specifically instrumented (Figure 1) for an Intensive Observation Period from June 1 to July 1, 1991. Atmospheric and hydrological variables were measured in addition to land-surface properties. Aircraft data were collected in order to provide large-scale integrated values of fluxes, which can give information on the spatial variability of the boundary layer in relation to surface inhomogeneities.

In this paper, we focus on a data set from a bare soil (Barrax site). Observations show very low water contents and high surface temperatures during the day, associated with large values of the net radiation and the sensible heat flux. Furthermore, the surface soil heat flux, which generally represents no more than 10% of the net radiation at the vegetation top, reaches 20 to 30% of the net radiation around noon in this case.

The prediction of the mass and energy budget on such a bare ground surface can be obtained using detailed models of the soil, describing all the physics of the processes. Such models require both a very high vertical resolution, especially close to the interface because of the high non-linearity of soil hydraulic properties, and very small time steps (to ensure the stability of the corresponding numerical scheme). The prediction of the time and space evolutions of the soil temperature and water content often needs coupled equations to be solved (Sasamori, 1970; Camillo *et al.*, 1983; Passerat *et al.*, 1989). The number of parameters necessary to describe the dependence of the thermal and hydraulic properties on the water

content and/or the temperature is large and these values are often only valid locally. All the requirements of detailed models are not compatible with the implementation within numerical weather prediction or general circulation models, where the computing time is limited and the area to be covered very large. Thus, simplifications are needed, limiting the number of predicted variables and the complexity of their predictive equations. The number of soil parameters is also reduced and they are often considered as dependent on soil texture; see for instance the Biosphere Atmosphere Transfer Scheme of Dickinson (1984), the Simple Biosphere model (Sellers *et al.*, 1986) or the scheme proposed by Noilhan and Planton (1989) (herafter NP89), derived from the Deardorff (1978) formulation.

The NP89 scheme, which is used in this study, has been extensively validated in the temperate zone using the Hapex–Mobilhy data set (Mahfouf and Jacquemin, 1989; Mahfouf, 1990; Jacquemin and Noilhan, 1990; Mahfouf and Noilhan, 1991). However, before the mesoscale modelling of the whole EFEDA region, local validations are needed, in order to see if some assumptions, valid under a temperate climate would not fail under dry conditions.

The main objectives of the study are:

(i) to analyse and discuss the data in order to set up a reference data set, suitable for both atmospheric and soil modelling studies;

(ii) to test and, if necessary, to improve the NP89 land-surface scheme in order to obtain better predictions of fluxes, soil temperature and water content over a bare dry soil.

2. The BARRAX Data Set

2.1. Atmospheric data

The Barrax site was equipped with a SAMER micrometeorological station (Automatic Station for the Measurement of Real Evapotranspiration). A description of the SAMER can be found in Goutorbe (1991). This station measures the mean atmospheric variables at a reference level $Z_a = 2$ m for the air temperature T_a and the specific humidity q_a and at $Z_v = 10$ m for the wind speed U_a and its direction. The net radiation R_n is deduced from the difference between downward and upward total radiation. The shortwave components are also recorded.

The SAMER station also measures the air temperature and wind speed at two levels (0.8 and 2.3 m, respectively). The sensible heat flux H is calculated using the aerodynamic method applied to these two levels (Itier, 1982). An iterative algorithm is used to deduce the friction velocity u_* and friction temperature θ_* from the wind speed and temperature differences between the two levels. Then H is computed as:

$$H = -\rho_a \cdot c_p \cdot u_* \cdot \theta_* , \tag{1}$$

where ρ_a is air density and c_p is specific heat.

For the surface soil heat flux G, two estimates are derived. The first one uses direct measurements of the ground heat flux with Thornthwaite plates, and the second one is based on a temperature series measured in the soil at 1 cm.

For the first estimate, the Thornthwaite plates measuring the ground heat flux were situated 5 cm beneath the surface. A correction of their value was performed in order to take account of the heat stored within the first 5 cm. The soil temperature just beneath the surface was measured approximately at 1 cm. The temperature gradient ΔT_s between the surface and $z_2 = 5$ cm was also available.

The heat stored in the soil between level z_1 and z_2 is given by (Fuchs and Tanner, 1968):

$$\Delta Q_s = \int_{z_1}^{z_2} c_g \frac{\partial T_s}{\partial t} \mathrm{d}z ,$$

where c_g is the volumetric heat capacity. A discretized estimate of this quantity was computed, assuming a linear temperature profile within the first 5 cm. Finally, the surface soil heat flux was computed as:

$$G = G_{(z = 5\text{ cm})} + c_g \Delta z \left(T_s^{t_1}(1\text{ cm}) - T_s^{t_0}(1\text{ cm}) + \frac{(\Delta T_s^{t_0} - \Delta T_s^{t_1})}{2} \right) \Big/ Dt , \tag{2}$$

where $\Delta z = 5$ cm, $Dt = 30$ min and t_0 and t_1 are two consecutive time steps. The coefficient c_g was taken as $c_g = 1.2 \times 10^6\ \mathrm{J\ m^{-3}\ K^{-1}}$. The second estimate of soil heat flux was derived, for each day, from the Fourier analysis applied to the soil temperature measured at 1 cm.

$$T_{\text{soil}}(1\text{ cm}) = Ao + \sum_{n=1}^{M} (A_n \cos(n\omega t) + \beta_n \sin(n\omega t)) , \tag{3}$$

where M is the number of harmonics and $\omega = 2\pi/\tau$ with $\tau = 1$ day. Then the soil heat flux at the surface is obtained as:

$$G = \lambda \left(\frac{\partial T_s}{\partial z} \right)_{(z=0)} \tag{4}$$

leading to:

$$G = \sqrt{2}\lambda \sum_{n=1}^{M} \exp(-z/d_n) d_n^{-1} \left[A_n \cos\left(n\omega t + \frac{\pi}{4} - \frac{z}{d_n} \right) + \right.$$

$$\left. + B_n \sin\left(n\omega t + \frac{\pi}{4} - \frac{z}{d_n} \right) \right] , \tag{5}$$

where $d_n = \sqrt{\tau\lambda/n\pi c_g}$ (Horton and Wierenga, 1983; Brunet, 1984; Passerat, 1986). Here, $z = -1$ cm, i.e., the depth at which T_s was measured, $\lambda = 0.42\ \mathrm{W\,m^{-1}\,K^{-1}}$ and $c_g = 1.2 \times 10^6\ \mathrm{J\,m^{-3}K^{-1}}$ (see also Section 2.2).

Finally, the latent heat flux is obtained as the residual of the surface energy budget:

$$LE = R_n - H - G\,. \tag{6}$$

Uncertainties in the latent heat flux can be estimated from an error analysis:

$$\frac{\Delta LE}{LE} = \frac{\Delta R_n}{R_n}\frac{R_n}{LE} + \frac{\Delta H}{H}\frac{H}{LE} + \frac{\Delta G}{G}\frac{G}{LE}\,. \tag{7}$$

The absolute error on R_n is $\pm 10\ \mathrm{W\,m^{-2}}$ (Bessemoulin, personal communication). From the two estimates of G (Figure 2), the absolute value for ΔG can be taken as $20\ \mathrm{W\,m^{-2}}$. The error in H is related to the absolute error in the measurements of the temperature and wind differences between two levels ($\pm 0.01C$ and $\pm 0.1\ \mathrm{m\,s^{-1}}$, respectively). The expressions given by Goutorbe (1991) lead to $\Delta H = 10\ \mathrm{W\,m^{-2}}$. So, during the daytime, if we consider that $R_n/LE \approx 6$, $H/LE \approx 4$ and $G/LE \approx 1$, the relative error in LE is 40%, which corresponds to uncertainties of $\pm 40\ \mathrm{W\,m^{-2}}$ for values of $LE \approx 100\ \mathrm{W\,m^{-2}}$. During the night, assuming that $R_n/LE \approx 6$, $H/LE \approx 1$ and $G/LE \approx 6$, we obtain $\Delta LE/LE \approx 400\%$, and again $\Delta LE = \pm 40\ \mathrm{W\,m^{-2}}$, since LE is about $10\ \mathrm{W\,m^{-2}}$. Note that the main source of uncertainty concerns the surface soil heat flux.

Table I shows the good agreement between the diurnal cumulative evaporation (between 8.00 and 16.00 GMT) obtained when the soil heat flux is deduced from the Thornthwaite plates (Equation (2)) or from the Fourier analysis (Equation (4)).

On the other hand, during the night or the late afternoon, signs can be changed between the two estimates. A negative latent heat flux (i.e., directed towards the surface and implying dew deposition), observed when G from the Thornthwaite plate is used in the surface energy budget (Figure 2), is unlikely to occur given the surface temperature at the end of the afternoon. Nevertheless, this phenomenon was also observed on the Gobi desert (Wang and Mitsuta, 1992), using eddy correlation techniques, even if the physical explanation remains to be found. In our case, the uncertainty on the LE sign during the night lies within the confidence interval of the data, and it is difficult to conclude which method is to be believed. The obvious consequence is a difference of 4 mm between the two estimates of cumulative evaporation over the 11 days (Figure 10), i.e., a relative error of about 25%.

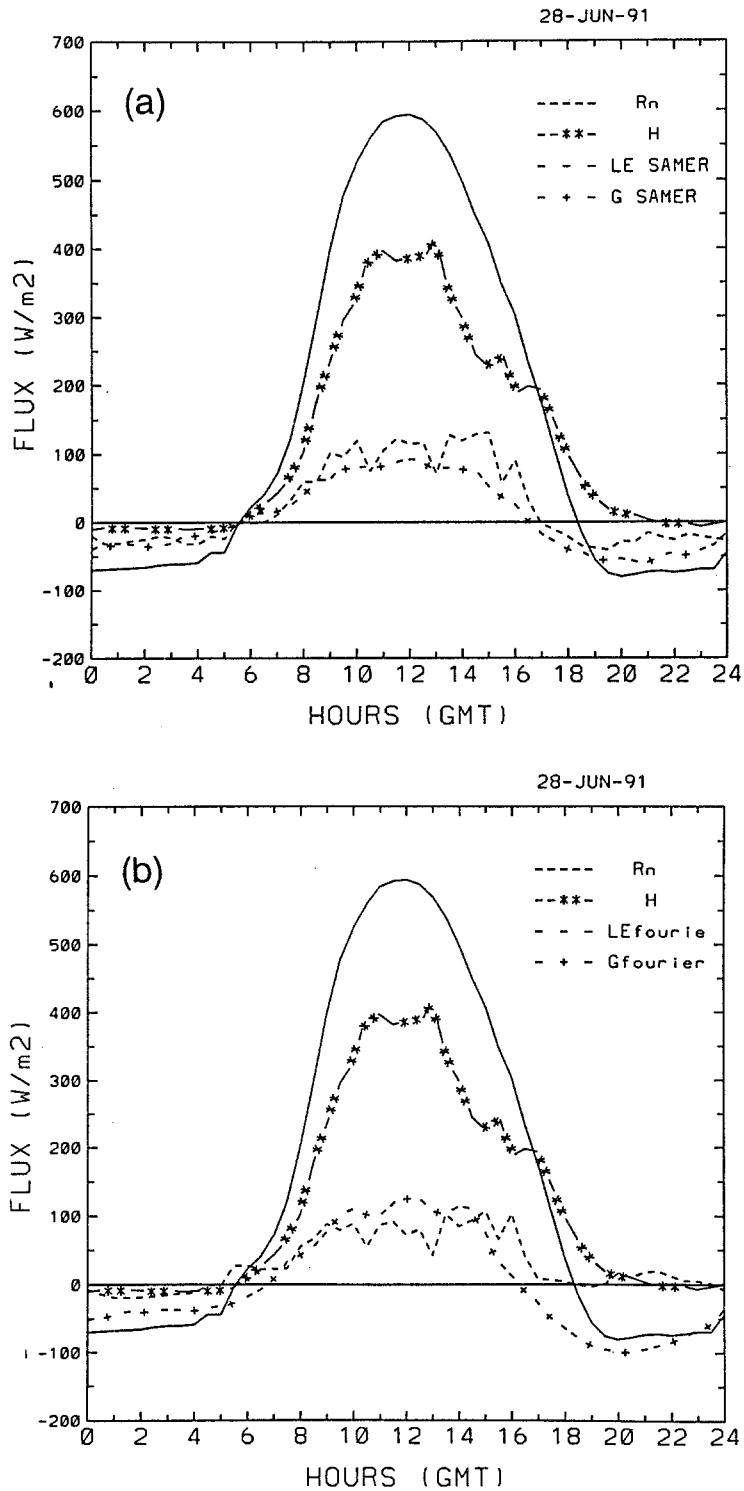

Fig. 2. Components of the energy budget for June 28, 1991 (a) when G is estimated using the Thornthwaite plate measurements and (b) when G is calculated using FOURIER series.

TABLE I

Daily diurnal cumulative evaporation (mm) computed between 8.00 UTC and 16.00 UTC. The "Thornthwaite" column corresponds to the observation when the soil heat flux is the corrected Thornthwaite plate measurement at 5 cm. The "Fourier" column shows the observed evaporation when the soil heat flux is estimated using Fourier series (see also text). The "model" column corresponds to the simulation with vapor phase parameterization and the use of separate roughness lengths for momentum and heat

Day	Thornthwaite	Fourier	Model
06/20	1.74	1.61	1.30
06/21	1.30	1.12	1.01
06/22	1.89	1.72	1.38
06/23	1.65	1.44	1.34
06/24	1.87	1.66	1.47
06/25	0.89	0.70	1.42
06/26	1.91	1.71	1.55
06/27	1.36	1.22	1.55
06/28	1.14	0.89	0.66
06/29	0.47	0.22	0.48
06/30	0.49	0.23	0.51
Total	14.71	12.52	12.67

2.2 Hydrological data and soil properties

a. *Textural Analysis*

Soil samples were taken, near the SAMER station at eight depths, regularly spaced between 0 and 85 cm. Their textural analysis was performed and the results are given on the textural triangle of Figure 3. Two horizons can be identified. Each of them was related to a soil type in the Clapp and Hornberger (1978) classification, the main characteristics of which are given in Table II. The first one (0–45 cm) corresponds to a silt loam (type 4) and the second one (45–85 cm) belongs to the fifth class (loamy soil) of that classification.

b. *Soil Thermal Properties*

Dry bulk density was deduced from the analysis of soil samples taken at Barrax. Combined with water content measurements using one neutron probe, it allowed for the calculation of the volumetric heat capacity c_g using the De Vries (1975) formula:

$$c_g = c\,\mathrm{dry} + 4.18 \times 10^6 w_g \tag{8}$$

with $c_g\,\mathrm{dry} = 0.78 \times 10^6\,\mathrm{J\,m^{-3}\,K^{-1}}$. For the correction of G using (2), w_g was taken as $0.10\,\mathrm{cm^3\,cm^{-3}}$, which is the mean value of the observed mean surface water content during the 11 days. In the vicinity of the SAMER station, the

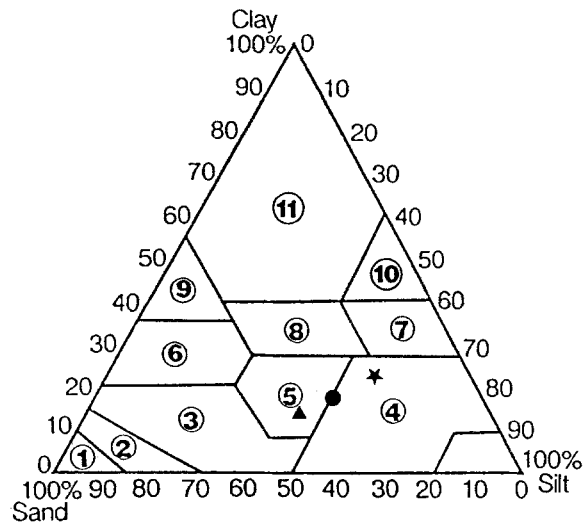

Fig. 3. Textural triangle giving the soil type for the 0–45 cm layer (star), the 45–85 cm layer (full triangle) and the 0–85 cm layer (full circle).

TABLE II

The soil types of the Clapp and Hornberger classification and their main characteristics

Soil type	w_{sat} ($cm^3\ cm^{-3}$)	h_{sat} (m)	K_{sat} ($10^{-6}\ m\ s^{-1}$)	w_{wilt} ($cm^3\ cm^{-3}$)	w_{fc} ($cm^3\ cm^{-3}$)	b
Sand	0.385	−0.121	176.0	0.068	0.135	4.05
Loamy sand	0.410	−0.090	156.3	0.075	0.150	4.38
Sandy loam	0.435	−0.218	34.1	0.114	0.195	4.90
Silt loam	0.485	−0.786	7.2	0.179	0.255	5.3
Loam	0.451	−0.478	7.0	0.155	0.240	5.39
Sandy clay loam	0.420	−0.299	6.3	0.175	0.255	7.1
Silty clay loam	0.477	−0.356	1.7	0.218	0.322	7.75
Clay loam	0.476	−0.630	2.5	0.250	0.325	8.52
Sandy clay	0.426	−0.153	2.2	0.219	0.310	10.4
Silty clay	0.482	−0.490	1.0	0.283	0.370	10.4
Clay	0.482	−0.405	1.3	0.286	0.367	11.4

thermal conductivity λ was also measured using the line source method (Laurent, 1989). Ten replications performed at about 20 cm depth lead to a mean value of $\lambda = 0.42\ W\ m^{-1}\ K^{-1}$ with a coefficient of variation of 23%, while the corresponding mean volumetric water content was $w_g = 0.15 \pm 0.02\ cm^3\ cm^{-3}$ at a soil temperature of 23.3C (Vauclin *et al.*, 1992). Unfortunately, in the absence of significant variations of w_g during the observation period, it was not possible to obtain a relationship between λ and w_g. Therefore, in the discussion below, λ will be kept at the one measured value.

c. *Water Content and Hydraulic Head Measurements*

Soil volumetric water content was measured at six levels, from 10 to 60 cm, using one neutron probe. Tensiometers were used to obtain the hydraulic head h at five levels (from 10 to 50 cm). When h is plotted as a function of the depth z, the depth of the zero flux plane can be determined. Then, the evaporation is calculated as the variation of the soil water content between two consecutive profiles, from the zero flux plane level to the surface (Vachaud *et al.*, 1981). In our case, the cumulative evaporation is only 2 mm from June 20 to June 30. Remember that the cumulative evaporation given by the SAMER is 12 to 16 mm for the same period and, therefore, the water balance between the atmosphere and the soil is not closed. No change in the water content was observed below 20 cm, due probably to the lack of sensitivity of the neutron probe for such low water content. The cumulative evaporation estimated from the soil measurements corresponds to a mean latent heat flux of 5–6 W m^{-2}. The mean amount of 14 mm deduced from atmospheric measurements leads to a mean value of about 40 W m^{-2}, with an uncertainty of ± 30 W m^{-2}. Therefore, the discrepancy between the two evaporation estimates seems mainly related to instrumental errors.

d. *Soil Hydraulic Properties*

Hydraulic properties can be characterized by two curves relating the pressure head h and the hydraulic conductivity to the water content. However, given the very dry conditions, values of the pairs (h, w) are only available for low water contents. Thus, it is very difficult to fit a curve to these data. The unsaturated hydraulic conductivity K_l was also measured using disk permeameters and the saturated hydraulic conductivity was measured with a Guelphpermeameter (Vauclin *et al.*, 1992). However, these data are still being processed, in order to obtain curves consistent with each other, and were not used in this study. The Clapp and Hornberger (1978) relationships given by (9) and (10) were used instead.

$$h(w) = h_{\text{sat}} \left(\frac{w_{\text{sat}}}{w} \right)^{b}, \tag{9}$$

$$K_l(w) = K_{\text{sat}} \left(\frac{w}{w_{\text{sat}}} \right)^{2b+3}, \tag{10}$$

h_{sat}, K_{sat} and b can be found in Table II for various soil types.

3. Modelling

A full description of the land-surface scheme used in the present study is given in Noilhan and Planton (1989). The full scheme is designed to represent the different components of the surface heat and moisture budget over various types of soil and canopies. Four prognostic variables are computed by the model: soil surface

temperature T_s, mean temperature of the soil column T_2, and two vertically averaged volumetric water contents:

(i) w_g, associated with a thin upper layer d_1, 1 cm thick;

(ii) w_2, which corresponds to the total soil depth d_2.

The deep water flux is assumed to be zero at depth d_2. The equations governing the evolution of these variables are given in Appendix 1, together with the calibration of the parameters versus the soil texture and water content. More specifically, the evaporation from the bare soil is expressed as a function of the difference between the specific humidity at the surface and at the reference level:

$$E_g = \rho_a \frac{h_u q_{\text{sat}}(T_s) - q_a}{r_a}, \tag{11}$$

where q_a is the specific humidity of the air at level z_a and $q_{\text{sat}}(T_s)$ the saturated specific humidity at temperature T_s. r_a is the aerodynamic resistance and h_u the relative humidity at the surface expressed empirically as a function of the surface volumetric water content w_g:

$$\begin{aligned} h_{\text{u}} &= 0.5\left(1 - \cos \pi \frac{w_g}{w_{fc}}\right) \quad \text{if } w_g \leqslant w_{fc} \\ h_{\text{u}} &= 1 \qquad\qquad\qquad\qquad \text{otherwise;} \end{aligned} \tag{12}$$

w_{fc} is the field capacity, corresponding to a hydraulic conductivity of 0.1 mm/day (see Jacquemin and Noilhan (1990) for its value as a function of the soil texture). Finally, the evolution of the surface volumetric water content is:

$$\frac{\partial w_g}{\partial t} = \frac{C_1}{\rho_w d_1}(P_g - E_g) - \frac{C_2}{\tau}(w_g - w_{geq}) \quad \text{for } w_g \leqslant w_{\text{sat}}. \tag{13}$$

Here, P_g is the rainfall, τ is a time constant of one day and ρ_w the density of liquid water. The coefficients C_1, C_2 and w_{geq} were expressed by NP89 as functions of soil texture and soil moisture, using formulations of Clapp and Hornberger (1978) (see Appendix 1). In Mahfouf and Noilhan (1991), several expressions for E_g were compared using *in situ* data from a bare soil. The bulk aerodynamic formulation (11) proved to give predictions of fluxes, temperatures and water contents matching the observations very well (see also Kondo *et al.*, 1990). Thus, the expression for E_g is not analysed further in this study and emphasis is put on the formulation of the coefficient C_1, which governs the evolution of the surface water content.

Schematically, the procedure used in this study is the following. At each time step, the model is forced using the atmospheric data (air temperature, specific humidity, wind speed) measured at the reference height and the observed global and atmospheric radiations. The coefficients, depending on the volumetric water content, are calculated using its value at the previous time step. Then, the equa-

TABLE III

Values of the parameters and initialisation of the prognostic variables. The stars indicate measured values and the method used to derive them is briefly given in the last column. The others are taken from the Clapp and Hornberger (1978) soil classification

Values of the parameters		
Total soil depth	$d_2 = 50$ cm	Position of the zero flux plane
Soil type	silt loam	Textural analysis
Saturated water content	$w_{sat} = 0.45\ cm^3\ cm^{-3}$	Dry bulk density measurements
Saturated hydraulic conductivity	$K_{sat} = 7.2 \times 10^{-6}\ m\ s^{-1}$	
Saturated hydraulic head	$h_{sat} = -0.786$ m	
Exponent of the $h(w)$ relationship	$b = 5.3$	
Field capacity	$w_{fc} = 0.255\ cm^3\ cm^{-3}$	
Wilting point	$w_{wilt} = 0.179\ cm^3\ cm^{-3}$	
Roughness length for momentum	$Z_o = 1$ cm	Wind and temperature "profiles"
Albedo	$\alpha = 0.23$	Difference between upward and downward radiations
Emissivity	$\epsilon = 0.97$	Nerry (1992)
Initial values of the prognostic variables (June 19 at 12.00 GMT)		
Surface temperature	$T_s = 40$ °C	Soil temperature at 1 cm
Deep temperature	$T_2 = 25$ °C	
Surface water content	$w_g = 0.10\ cm^3\ cm^{-3}$	Neutron probe
Deep water content	$w_2 = 0.20\ cm^3\ cm^{-3}$	Neutron probe

tions giving the four prognostic variables are solved, and the fluxes R_n, H, LE and G are deduced. Finally, the predicted temperatures, water contents and fluxes are compared to the observations.

3.1. Values of the parameters and initialisation of the simulation

Initial conditions of the simulations described in this paper are provided in Table III. Surface parameters were prescribed using observations when available. The roughness length Z_0 was derived from wind and temperature profile measurements (only two levels) using a least-squares technique. Only observations corresponding to a wind speed U_a higher than $4\ m\ s^{-1}$ and a Richardson number near zero ($|Ri| < 0.01$) were considered for this estimation (152 values). Concerning initial values of the prognostic variables, the initial value of the deep water content w_2 is most important because it evolves very slowly with time. Thus it determines to a large extent the prediction of the Bowen ratio. Therefore, it is very important to initialize the model reservoirs with observations of the soil water content in order to obtain a relevant calibration of the land-surface scheme.

In a first test, special attention was paid to the prediction of the surface soil heat flux G. When measurements of the soil thermal properties are not available, the C_G coefficient (Equation (A-7)) is calculated using formulas taken from Al Nakshabandi and Konkhe (1965) for the thermal conductivity λ and from De Vries (1975) for c_g. In NP89, a calibration of C_G, as a function of the soil texture

and water content is proposed. These formulas lead to an overestimation of the surface soil heat flux during the day (Figure 4a). On the other hand, when the measured λ and c_g are used in the model, the predicted G is reduced by 30% around midday and agrees fairly well with the observations (Figure 4b). The use of the Van de Griend and O'Neill (1986) relationships for $\sqrt{\lambda c_g}$, using the Clapp and Hornberger (1978) classification, also leads to an overprediction of G (not shown). A similar discrepancy was also observed by Mahfouf and Noilhan (1991) on a plot of silty clay loam soil, addressing the issue of the relevance of averaged thermal parameters in soil classifications when compared with observations. On the other hand, we must also emphasize that the Barrax soil, due to a particular agricultural work, had a very low dry bulk density, leading probably to specific thermal properties.

Nevertheless, the use of the measured values of the thermal properties provided a great improvement of model results and allowed us to reduce a major uncertainty in the soil heat flux prediction. Then, two weaknesses of the model under the dry conditions reported in this study were investigated:

(i) The surface temperature was underpredicted around noon, leading to an overprediction of net radiation. The influence of the value of the ratio between the roughness lengths for momentum and heat transfers on the predicted surface temperature was thus examined.

(ii) A low evaporation rate at the end of the observing period was not correctly reproduced. This led to the parameterization of the vapour phase transfer, which was neglected in the original model version.

These two points are now developed in the following subsections.

3.2. Improvements of the surface temperature prediction

a. *Experimental and Theoretical Background*

At Barrax, only the soil temperature at 1 cm was measured. Thus, the quality of the prediction of the surface temperature was evaluated from comparison between the observed and predicted net radiation. Indeed, the global and infrared radiations, as well as the albedo and the emissivity were measured. Therefore, any discrepancy between the observed and predicted R_n can be explained by an erroneous specification of surface temperature. Uncertainties concerning the thermal properties of the soil were limited, due to the use of measured values.

Thus, we examined the values of the roughness lengths for heat and momentum. Experimental and theoretical work has shown that these values are, in general, different. For instance, using wind tunnel measurements, Owen and Thomson (1963) expressed the ratio Z_o/Z_{oh} as a function of the roughness Reynolds number R_e^* and of the Prandtl number (see also Brutsaert 1975, 1982). Using data taken from various experiments, Garratt and Hicks (1973) showed that this relation matched the observations fairly well for R_e^* lower than 100, but for higher R_e^*, which occurs on natural surfaces, the dependence of Z_o/Z_{oh} on R_e^* does not appear

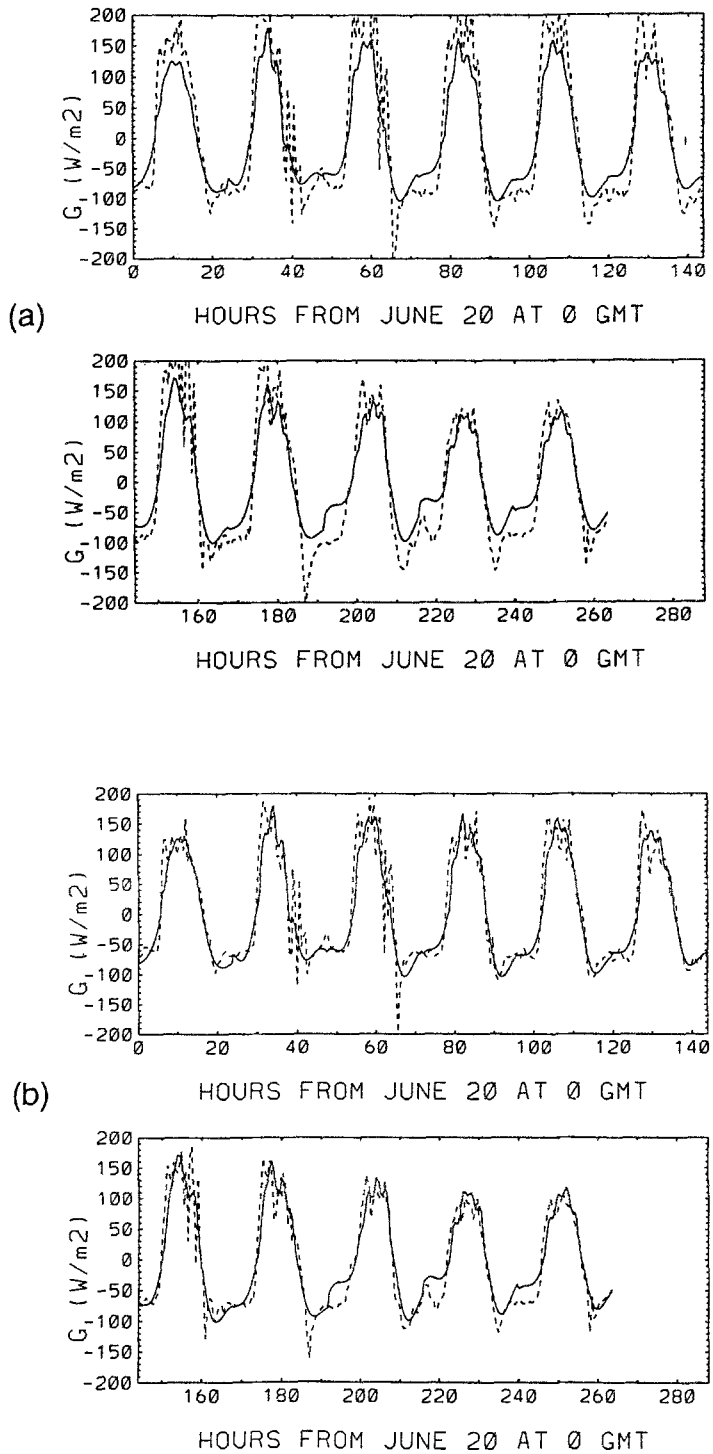

Fig. 4. Comparison of the soil heat flux time evolution predicted by the model (dotted line) with the observations deduced from the Fourier series (solid line) when (a) the thermal properties are derived from the soil type and (b) the measured thermal properties are used.

to be unique. Recently, Duynkerke (1992) reported a strong dependence of Z_o/Z_{oh} on the friction velocity for soil covered by short grass. On the other hand, the ratio was found nearly independent of R_e^* in other cases. For instance, Garratt (1978) obtained a ratio $Z_o/Z_{oh} = 12$ from observations on a natural area composed of forest, crop and grassland. In the literature, values ranging from 3 to 10–12 are reported. Furthermore, these studies were not able to give evidence of the difference between the roughness lengths for heat and vapour. They are assumed to be equal in this paper.

The roughness lengths for momentum and heat appear in the aerodynamic resistance used in the expression of the sensible and latent heat flux (see Equation (A-9) and (11)). The expression of r_a is derived from the similarity theory of Monin and Obukhov (1954):

$$r_a = \frac{[\ln Z_a/Z_{oh} - \Psi_h(Z_a/L)][\ln Z_a/Z_o - \Psi_m(Z_a/L)]}{k^2 U_a}, \tag{14}$$

Ψ_m and Ψ_h are the Paulson stability functions (Paulson, 1970), L is the Monin–Obukhov length and k the Karman constant.

b. *Results of the Simulation*

The length Z_{oh} could not be inferred from our data set because the skin temperature was not available. Only the soil temperature at 1 cm was measured. Thus, Z_{oh} was tuned in order to match the observed net radiation (Figure 5b). We obtained $Z_{oh} = 1$ mm which leads to a ratio $Z_o/Z_{oh} = 10$. This value agrees with those reported in the literature. On the other hand, with $Z_0/Z_{oh} = 1$, the net radiation was overestimated around noon (Figure 5a).

When a ratio $Z_o/Z_{oh} = 10$ is used, a fair prediction of the sensible heat flux results (Figure 6). We also checked that the predicted T_s was compatible with the soil temperature measured at 1 cm, $T_{\text{soil}}(1\text{ cm})$. The latter quantity is indeed out of phase with T_s and has a dampened amplitude (Brunet, 1984, for instance). Figure 7 shows that the predicted T_s exhibits a maximum value comparable to or higher than that of $T_{\text{soil}}(1\text{ cm})$. It is not the case with $Z_o = Z_{oh} = 1$ cm, where T_s has a smaller amplitude than $T_{\text{soil}}(1\text{ cm})$.

To investigate the sensitivity of the prediction of T_s as a function of the value of Z_{oh}, several tests were performed. When Z_{oh} decreased from 1 cm to 0.1 mm, the maximum surface temperature varied from 51.2 to 62.3 °C. The effect on the minimum surface temperature was much less, and the corresponding variation of T_s was from 11.1 to 11.5 °C. This behaviour is probably due to the fact that the nocturnal evolution of T_s depends mainly on the soil thermal inertia and not on atmospheric conditions. Furthermore, when Z_{oh} was decreased, so did the sensible heat flux H. It meant that, according to (A-9), the increase of $(T_s - T_a)$ was slower than the increase in the atmospheric resistance r_a.

In conclusion, the calibration of the NP89 scheme for dry bare-soil leads to a

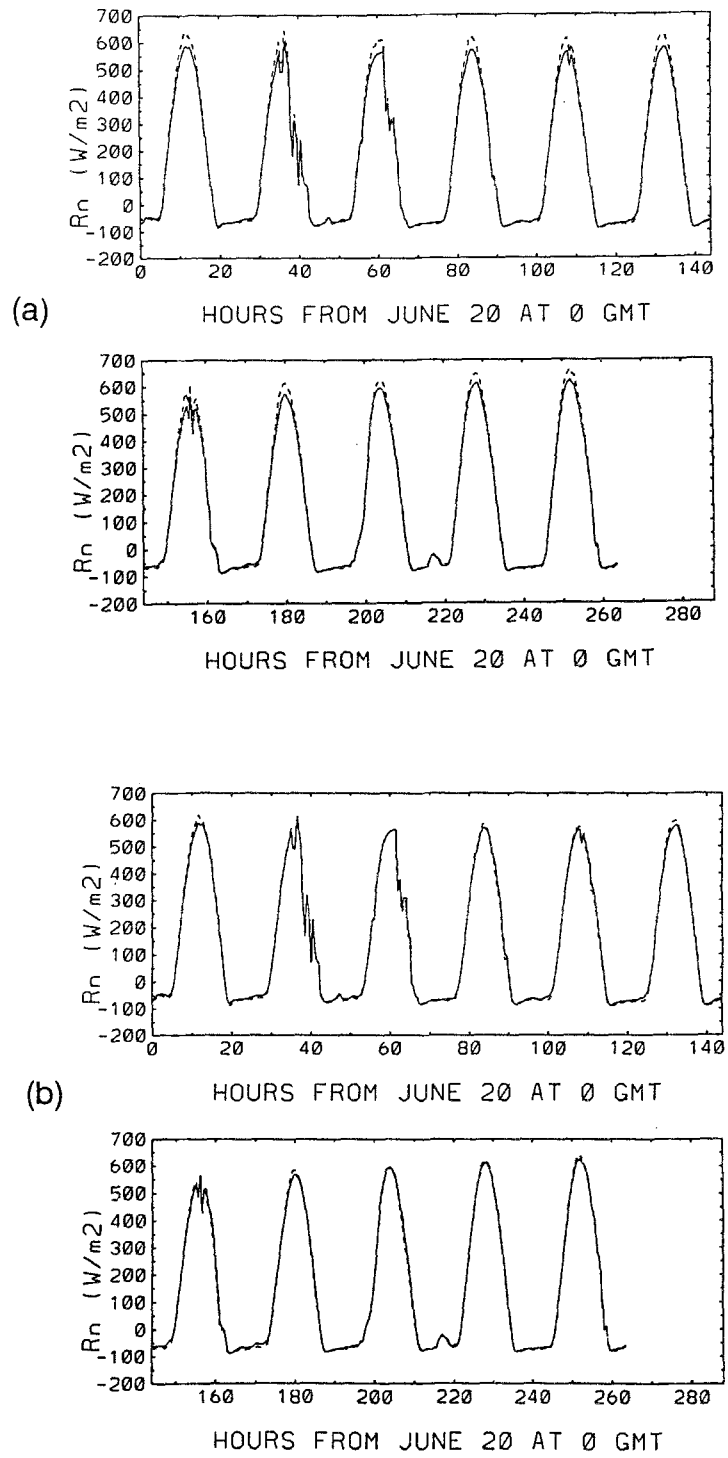

Fig. 5. Comparison of the predicted net radiation time evolution (dotted line) when (a) $Z_o = Z_{oh} =$ 1 cm and (b) $Z_o = 1$ cm and $Z_o = 1$ mm with the observed net radiation (solid line).

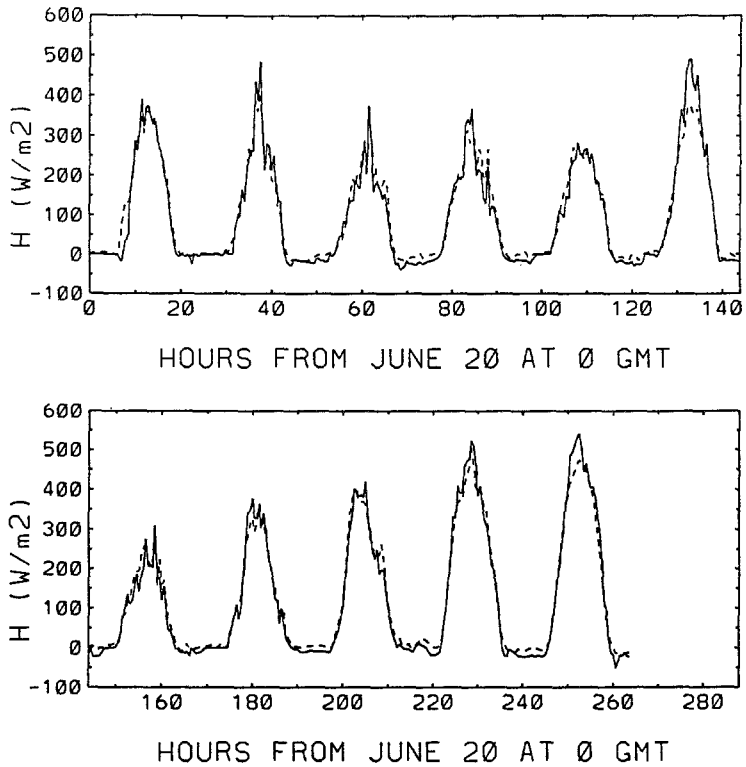

Fig. 6. Time evolution of the predicted sensible heat flux for $Z_o = 1$ cm and $Z_{oh} = 1$ mm (dotted line) and of the observed sensible heat flux (solid line).

ratio of $Z_o/Z_{oh} = 10$ in agreement with numerous studies. If the roughness lengths are taken to be equal, as is often assumed in atmospheric modelling, a poorer prediction of surface temperature results. We must also mention that the sensitivity to the specification of the soil hydraulic properties was examined, and the results showed that the main conclusions given below are valid. This remark also holds for the following subsection.

3.3. Introduction of water phase transfer into the parameterization

In the model, C_1 is the coefficient which mainly governs the surface water content evolution as can be seen from (13). C_1 was parameterized, using Equation (A-8), as a function of the soil texture and of the surface water content. Nevertheless C_1 was limited to a maximum value $C_{1\max} = C_1(w_{\text{wilt}})$ for water contents below the wilting point w_{wilt}. For silt loam, $C_{1\max} = 1.12$. In the simulations, given the low moisture content, C_1 was always set to this maximum and remained constant all the time. The cumulative evaporation obtained in this case was much smaller than the observed value. To match the observations, $C_{1\max}$ had to be changed and an optimum of $C_{1\max} = 0.45$ was found. This corresponds to a penetration depth of

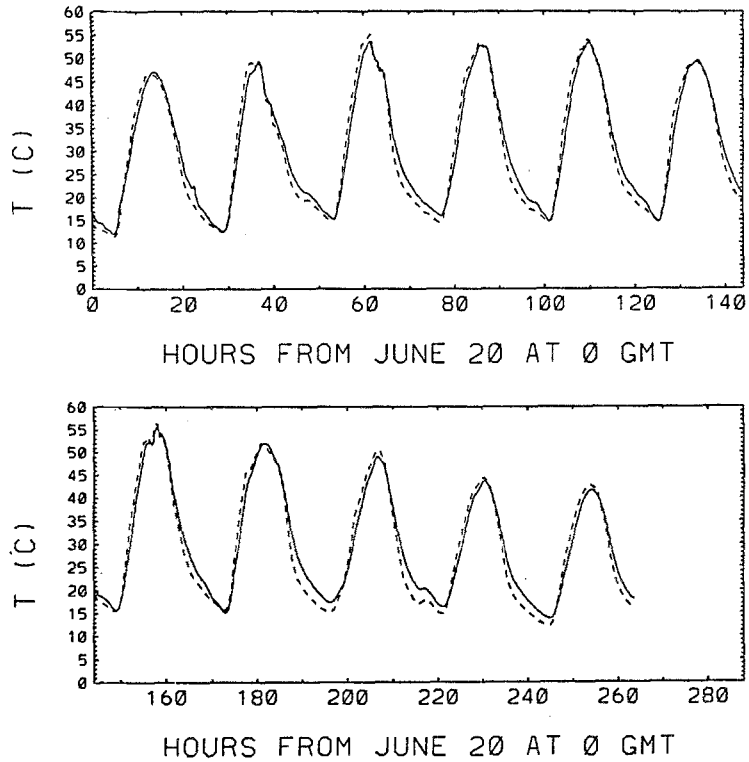

Fig. 7. Comparison of the time evolution of the predicted surface temperature T_s with $Z_o = 1$ cm and $Z_{oh} = 1$ mm (dotted line) with the measured soil temperature at 1 cm (solid line).

the diurnal cycle of about $d = 4.4$ cm. This tuning is possible only when measurements of the evaporation are available and is probably only valid locally. The extension of this procedure to operational models is not possible given the lack of measurements over large areas. Furthermore, it is not satisfactory from a physical point of view.

Given the very low water contents and the high temperature during the day, the dominant transfer mode is the vapor phase. Indeed, the vapor diffusivity is higher than the liquid diffusivity (Jackson *et al.*, 1974; Menenti, 1984). In the original version of the NP89 scheme, only liquid transfer is taken into account. C_1 was thus modified to include vapor phase transfer. This modification has been made keeping in mind that the parameterization should be as simple as possible, and computationally not excessive. Therefore, the introduction of an explicit coupling between the water content and temperature equations is avoided. In fact, only vapor transfer due to the pressure gradient is included in the evolution of the surface water content w_g. This choice is discussed below. First of all, we concentrate on the theoretical and practical aspects of this parameterization, and then comment on the results of the simulation.

a. *Parameterization of Vapor Phase Transfers*

The approach is based on the analytical solution of a simplified pressure head equation which includes vapor transfer due to a pressure gradient (Appendix 2). This calculation leads to a new expression for C_1:

$$C_1 = 2d_1\sqrt{(\pi c_w)/\tau(K_l + D_{vh}/\rho_w)}\,, \tag{15}$$

where D_{vh} is the isothermal vapor conductivity (Appendix 2, Equation (A-12)). K_l and D_{vh} are functions of the soil texture and water content and, in addition, D_{vh} also depends on the soil temperature (Equation (A-12)). Therefore, C_1 is parameterized as a function of the soil type, the surface water content w_g and temperature T_s. Figure 8 provides the evolution of C_1 as a function of the volumetric water content for the Barrax soil and for a typical clay soil taken from the Clapp and Hornberger classification. Several values of the temperature T_s are considered. The value of C_1 using the original scheme is also shown (dotted line). With the new formulation given by (15), three parts of the curves can be distinguished. For $w_g > w_{\text{wilt}}$, we have $K_l \gg D_{vh}/\rho_w$ and transfer occurs in the liquid phase. These parts of the curves do not depend on the temperature. For low water contents, $D_{vh}\rho_w \gg K_l$ and transfer occurs in the vapor phase. In the intermediate range of water content, both types of transfer are of the same order of magnitude. When vapor phase transfer is dominant (left-hand side parts of the curves), C_1 decreases when the surface temperature increases. It means that the depth d, involved in the vapor phase transfer, increases. Finally, it seems that fine soil textures such as clay (Figure 8b), are more likely to experience vapor phase transfer, because their wilting point is higher. However, data from such soils would be necessary to confirm this remark.

b. *Result of the Simulation When Vapor Phase is Included*

The evolution of C_1 during the 11 day simulation is given in Figure 9. It is worth noting that C_1 can range from 0.2 to 2.5, and most of the transfer occurs effectively in the vapor phase. With the previous formulation of C_1, it was systematically set to its maximum value calibrated as $C_{1\max} = 0.45$. The new parameterization leads to a comparable cumulative evaporation (Figure 10), but C_1 evolves freely in the simulation, without any arbitrary preset maximum value. This is much more physically based and satisfactory for operational use. In addition, the comparison of Figure 10a (original C_1 formulation) and 10b (modified C_1 formulation) shows that the low evaporation during the last three days is predicted better with the vapor phase transfer. Note also that the predicted model evaporation lies between the two estimates deduced from the data. The major discrepancies are observed during the night, where the model sets the evaporation to zero. Indeed, we used here the proposal of Mahfouf and Noilhan (1991) which prevents dew deposition when $q_{\text{sat}}(T_s) > q_a$, even if $h_u q_{\text{sat}}(T_s) < q_a$. Thus, further studies and measurements are needed to validate this part of the model. However, if we restrict the compari-

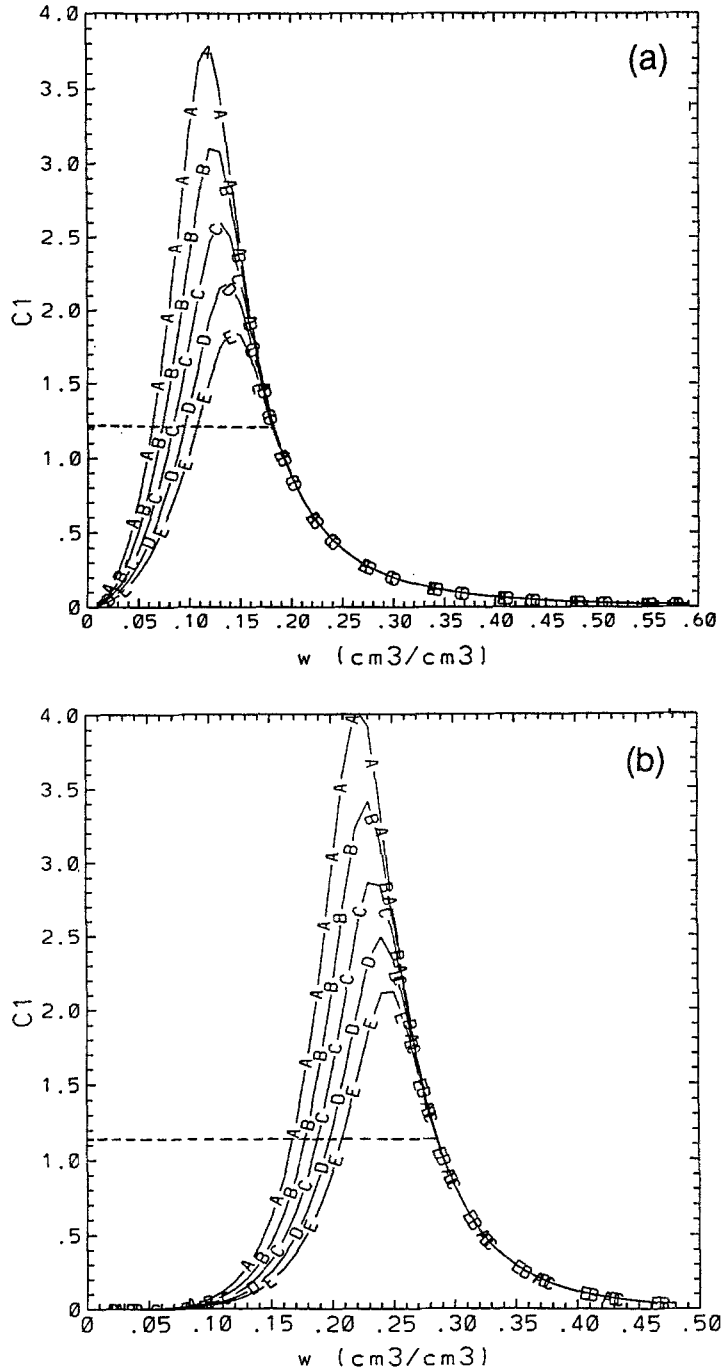

Fig. 8. C_1 coefficient versus soil volumetric water content for several values of the surface temperature T_s for (a) the Barrax soil and (b) a typical clay soil of the Clapp and Hornberger classification. (-A-): T_s = 10C, (-B-): T_s = 20C, (-C-): T_s = 30C, (-D-): T_s = 40C, (-E-): T_s = 50C. The dotted lines correspond to the initial parameterization when only liquid transfer was considered.

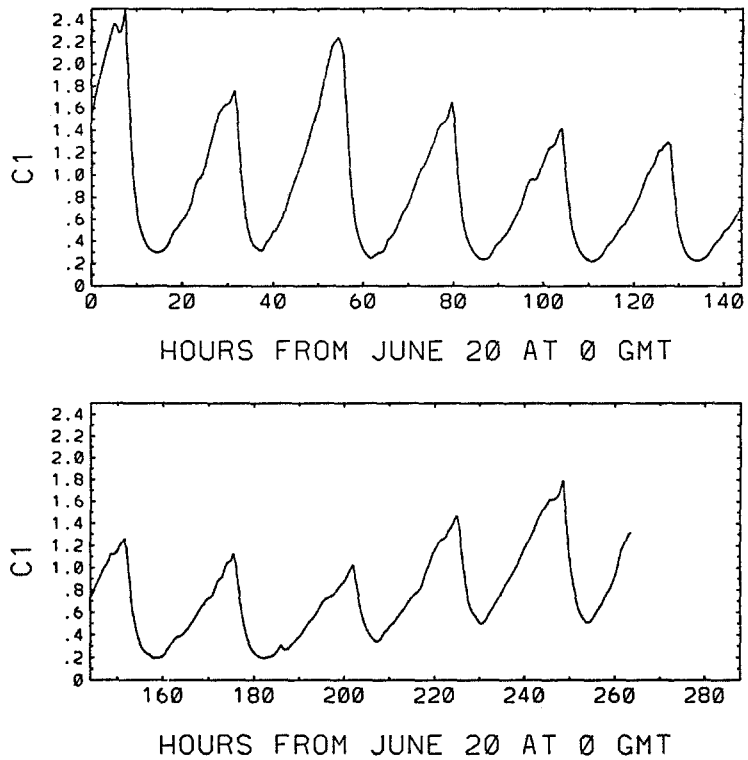

Fig. 9. Time evolution of C_1 when vapor phase transfer is included.

son between the observations and the model results to the daytime (Table I), a satisfactory agreement between predicted and observed (using the Fourier method) mean daily evaporation is obtained. In terms of water content, Figure 11 provides the evolution of the surface and deep water contents. Neutron probe measurements are also given and their values agree reasonably well with the model predictions. However, surface measurements are too sparse in time to allow for the validation of the predicted diurnal cycle. On the other hand, neutron probe observations show that the observed mean water content remains almost constant during the period, whereas the predicted w_2 decreases slowly. This behaviour is consistent because, in the model, the deep reservoir is closed and its level decreases to supply the evaporative demand. We already pointed out that the cumulative evaporation deduced from the neutron probe measurement is only 2 mm over the 11 days and that the discrepancy found between the observed soil water budget and the atmospheric evaporation cannot be explained satisfactorily.

c. *Comment on the Modified Parameterization of* C_1

For the assessment of the new parameterization of C_1, several assumptions were made. More specifically, transfers due to temperature gradients were neglected.

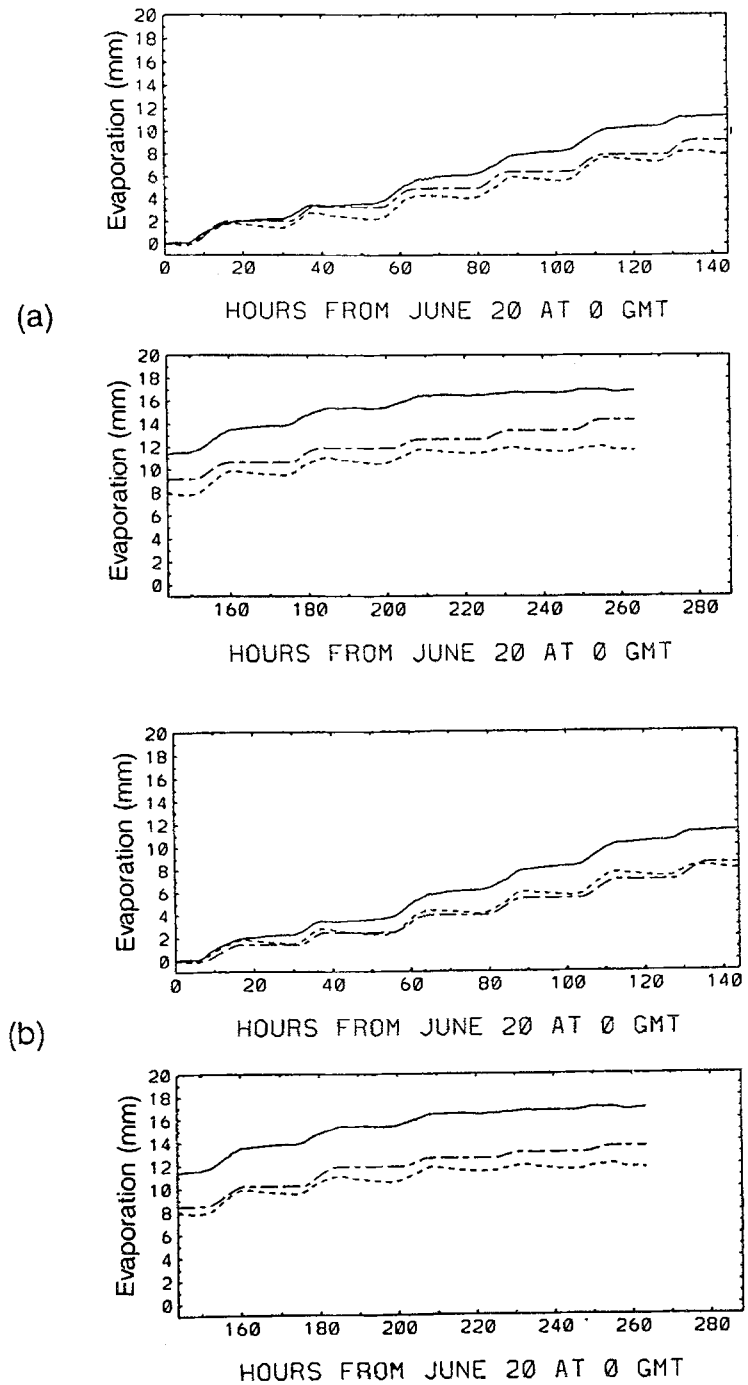

Fig. 10. Comparison of the time evolution of the observed cumulative evaporation (solid line for the Thornthwaite estimate and dotted line for the Fourier estimate, see also text) with the predicted cumulative evaporation (broken line) when (a) only liquid transfer is included and (b) when vapor phase transfer is added.

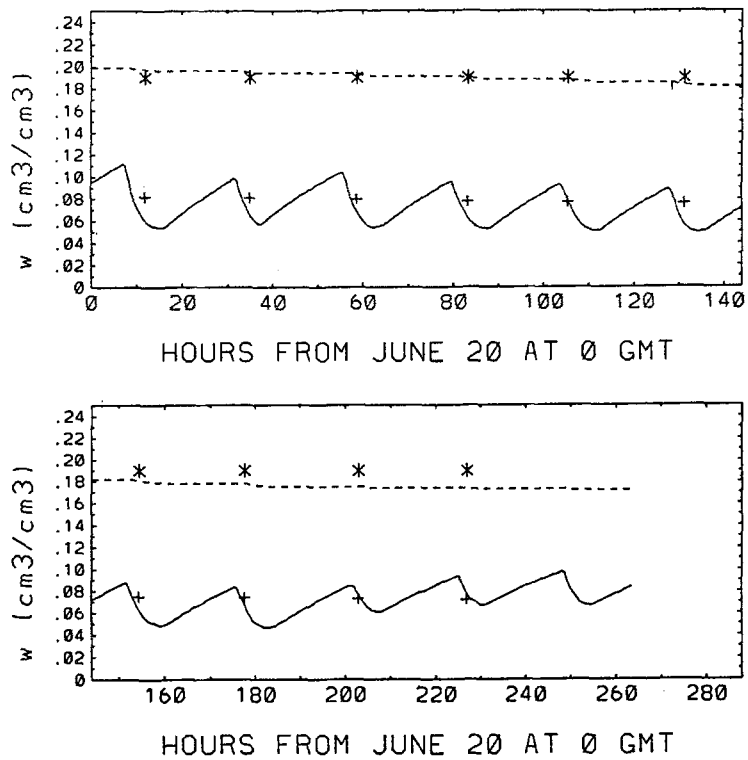

Fig. 11. Time evolution of the predicted surface (solid line) and deep (dotted line) volumetric water contents. Crosses are neutron probe measurements at 10 cm and stars are means of neutron probe values within the first 50 cm.

However, they may be of the same order of magnitude as transfers due to pressure gradients. To discuss this point a detailed model would be needed. However, as the coefficient D_{vh} was parameterized as a function of T_s, we can assume that the role of temperature gradients is implicitly included. Furthermore, the results of the simulation using (15) fit the observations. Therefore, we can assume that the underlying physics is correctly reproduced.

4. Conclusions

This paper presents a validation of the NP89 land-surface parameterization under the very dry conditions and high daytime temperatures of the 1991 EFEDA experiment. Local measurements of the thermal soil properties were directly introduced into the model, allowing for a fair prediction of the surface soil heat flux, which was an important term of the daytime surface energy budget. In the original version of the NP89 scheme, it was found that the soil thermal properties obtained from Al Nakshabandi and Konhke (1965) or Van de Griend and O'Neill

(1986) led to an overprediction of the surface ground heat flux. This addresses the issue of the relevance of averaged values in soil classification. After calibration of the soil thermal transfer, the study concentrated on two weaknesses in the original version of the model under these dry conditions:

(i) A value of 10 for the ratio between the roughness lengths for momentum and heat was determined to be necessary in order to correctly predict the surface temperature. The value of this ratio must now be confirmed by further studies over sparse vegetation canopies.

(ii) Given the very low water contents, the introduction of vapor phase transfer was necessary to reproduce the physics of the water exchange. A parameterization of vapor phase transfer due to pressure gradients is proposed as a function of the soil texture, the surface water content and temperature. The results obtained in terms of evaporation and water content are consistent enough with the observations to support the proposed simplified approach.

Thus, to reproduce the physics of heat and water transfers in extreme conditions on a bare soil, improvements of the original scheme proved necessary at the local scale. In the case of mesoscale meteorological models or GCMs, the question of generalization of these improvements may be discussed. Vapor phase transfer is probably the easiest to implement because the calculation of the isothermal vapor conductivity only needs to be performed for water contents lower than the wilting point and, furthermore only requires values of parameters or variables already calculated by the model. The case of the roughness lengths is more difficult to handle. Indeed, a specification of the ratio Z_o/Z_{oh} would have to be prescribed for several types of soil and vegetation covers. Some results have already been published but additional studies are probably necessary to cover all types of landscape. Finally, as in Mahfouf and Noilhan (1991), the problem of dew deposition was not solved because more accurate and specific measurements would be necessary to validate the parameterization. The study also underlined the great difficulty in getting accurate estimates of the various terms of the surface energy balance and water budget with conventional operating systems (i.e., SAMER, neutron probe) under very dry conditions. Therefore, more attention should be paid in the future to the measurements of the water cycle components when the variations are of the same order of magnitude as the accuracy of the sensors.

Appendix 1: The Land-Surface Parameterization of Noilhan and Planton (1989)

The equations giving the evolution of the prognostic variables are:

$$\frac{\partial T_s}{\partial t} = C_G(R_n - H - LE) - \frac{2\pi}{\tau}(T_s - T_2)\,, \tag{A-1}$$

$$\frac{\partial T_2}{\partial t} = \frac{1}{\tau}(T_s - T_2)\,, \tag{A-2}$$

$$\frac{\partial w_g}{\partial t} = \frac{C_1}{\rho_w d_1}(P_g - E_g) - \frac{C_2}{\tau}(w_g - w_{geq}) \quad \text{for } w_g \leqslant w_{\text{sat}}\,, \tag{A-3}$$

$$\frac{\partial w_2}{\partial t} = \frac{1}{\rho_w d_2}(w_g - w_2) \quad \text{for } w_g \leqslant w_{\text{sat}}\,; \tag{A-4}$$

P_g is the rainfall and E_g the evaporation from bare soil. τ is a time constant of one day and ρ_w the density of liquid water. C_2 and w_{geq} are computed as functions of the water content and the soil texture:

$$C_2 = C_{2\text{ref}} \frac{w_2}{w_{\text{sat}} - w_2 + w_{fc}}\,, \tag{A-5}$$

$$\frac{w_{geq}}{w_g} = \frac{w_2}{w_{\text{sat}}} - a\left(\frac{w_2}{w_{\text{sat}}}\right)^p \left(1 - \left(\frac{w_2}{w_{\text{sat}}}\right)^{8p}\right). \tag{A-6}$$

C_G represents the thermal capacity of the soil. If constant thermal properties of the soil and a sinusoidally varying soil heat flux $G = R_n - H - LE$ are assumed, T_s can be calculated and C_G is given by:

$$C_G = 2\sqrt{\frac{\pi}{\lambda c_g \tau}}\,, \tag{A-7}$$

where λ is the thermal conductivity of the soil and c_g its volumetric heat capacity. In the same way, if soil hydraulic properties are assumed to be homogeneous, the time evolution of w_g can be described similarly to the surface temperature. More specifically, C_1 is expressed as:

$$C_1 = 2d_1/d = 2d_1\sqrt{\frac{\pi|c_w|}{\tau K_l}}\,, \tag{A-8}$$

where $c_w = \partial w/\partial h$ is the capillary capacity, h, the matrix potential and K_l the hydraulic conductivity of the soil. d is the depth reached by the diurnal water content cycle. The values of the numerical coefficients a, b, p, $C_{G\text{sat}}$, $C_{2\text{ref}}$, w_{fc} and w_{sat} can be found in Jacquemin and Noilhan (1991).

The sensible heat flux is expressed as a function of the temperature gradient between the surface and the reference level:

$$H = \rho_a c_p (T_s - T_a)/r_a\,, \tag{A-9}$$

where ρ_a is the air density, c_p the specific heat of air, T_a the air temperature at the reference level Z_a and r_a the aerodynamic resistance. The evaporation formulation is presented in the text (Equations (11) and (12)).

Appendix 2: Derivation of the Coefficients When Vapor Phase Transfer is Included

The approach developed in Appendix of NP89 is used, but a modified pressure head equation is considered. Indeed, if the soil hydraulic properties are assumed to be homogeneous and only transfers due to pressure gradients are taken into account, this equation can be written:

$$c_w \frac{\partial h}{\partial t} = \left(K_l + \frac{D_{vh}}{\rho_w} \right) \frac{\partial^2 h}{\partial z^2}, \tag{A-10}$$

where h is the pressure head, z the vertical coordinate and D_{vh} the isothermal vapor conductivity. For a sinusoidal surface water flux with a one-day period, an exact solution of (A-10) can be found. This provides a new expression for C_1:

$$C_1 = 2d_1 \sqrt{\frac{\pi c_w}{\tau(K_l + D_{vh}/\rho_w)}}, \tag{A-11}$$

The coefficient C_1, which governs the surface water content evolution was parameterized as a function of w_g and T_s. An expression of the diffusion coefficient D_{vh} was also needed. D_{vh} is associated with the diffusion of vapor within the "dry" pores of the soil matrix and this process is enhanced by high soil temperatures. This coefficient is very difficult to measure. Laboratory techniques can be used (Bruckler *et al.*, 1989), but were not performed in this study. Therefore, the expression for D_{vh} was taken from the theory of Philip and De Vries (1957), and further development from Passerat *et al.* (1986).

$$D_{vh} = \frac{\alpha p}{(p - p_v(T_s))} \frac{D_{va}(T_s) F(n - w_g) g p_v(T_s)}{(RT_s)^2}, \tag{A-12}$$

where $\alpha = 0.66$ is a tortuosity factor, p the total air pressure, $p_v(T_s)$ the vapor pressure of the air near the surface at temperature T_s, R the gas constant for water vapor, g the acceleration of gravity, n the soil porosity and $D_{va}(T_s)$ the molecular diffusion coefficient of vapor water into the air given by:

$$D_{va}(T_s) = c^* \frac{p_o}{p} \left(\frac{T_s}{T_o} \right)^{n^*} \tag{A-13}$$

with $c^* = 2.17 \times 10^7$ m^2/s, $n^* = 1.88$ and $T_o = 273.16$ K.

Finally

$$F(n - w_g) = (n - w_g)[1 + w_g(n - w_{gk})^{-1}] \quad \text{for } w_g > w_{gk}$$
$$F(n - w_g) = n \quad \text{for } w_g < w_{gk};$$

w_{gk} is the critical water content which defines the loss of continuity of the liquid phase within the pores and $F(n - w_g)$ expresses the difficulty of vapor movement when liquid water increases within the pores. w_{gk} is textural dependent (De Vries,

1963) and was taken as $w_{gk} = 0.05\,cm^3/cm^3$ for the Barrax soil. At the surface (first 10 cm), the measured dry bulk density lead to a value of the porosity equal to $n = 0.66$. The corresponding saturated water content was thus set to 0.59 (90% of the porosity). These values were used to calculate the C_1 coefficient, which is representative of the surface properties.

Acknowledgement

This work was performed in the framework of the "Echival Field Experiment in a Desertification Threatened Area" project, funded by the European Community (Contract EPOC-CT90-0030) coordinated by H. J. Bolle (Freie Universität Berlin). The authors would particularly like to thank their colleagues at CNRM/4M and at LTHE, who provided them with the field data. O. Persson carefully reviewed the manuscript.

References

Al Nakshabandi, G. and Konkhe, H.: 1965, 'Thermal Conductivity and Diffusivity of Soils as Related to Moisture Tension and Other Physical Properties', *Agric. Meteorol.* **2**, 271–279.

André, J. C., Goutorbe, J. P. and Perrier, A.: 1986, 'HAPEX MOBILHY, a Hydrological Atmospheric Experiment for the Study of Water Budget and Evaporation Flux at the Climatic Scale', *Bull. Amer. Meteorol. Soc.* **67**, 138–144.

Bolle, H. J., Andre, J. C., Arrue, J. L., Barth, H. K., Bessemoulin, P., Brasa, A., De Bruin, H. A. R., Cruces, J., Dugdale, G., Engman, E. T., Evans, D. L., Fantechi, R., Fiedler, F., van de Griend, A., Imeson, A. C., Jochum, A., Kabat, P., Kratzsch, T., Lagouarde, J. P., Langer, I., Llamas, R., Lopez Baeza, E., Melia Miralles, J., Muniosguren, L. S., Nerry, F., Noilhan, J., Oliver, H. R., Roth, R., Saatchi, S. S., Sanchez Diaz, J., de Santa Olalla, M., Shuttleworth, W. J., Sögaard, H., Stricker, H., Thornes, J., Vauclin, M., and Wickland, A.: 1993, 'EFEDA: European Field Experiment in a Desertification Threatened Area', *Annales Geophysicae* **11**, 173–189.

Bruckler, L., Bell, B. C. and Renault, P.: 1989, 'Laboratory Estimation of Gas Diffusion Coefficient and Effective Porosity in Soils', *Soil Science* **147**(1), 1–10.

Brunet, Y.: 1984, 'Modélisation des échanges sol-nu atmosphère. Essai de validation locale et influence de la variabilité spatiale du sol', Ph.D. thesis. Université Scientifique et Médicale de Grenoble, Grenoble, France.

Brutsaert, W. H.: 1975, 'The Roughness Length for Water Vapor, Sensible Heat and Other Scalars', *J. Atmos. Sci.* **32**, 2028–2031.

Brutsaert, W. H: 1982, *Evaporation into the Atmosphrere. Theory, History and Applications*', D. Reidel Publishing Company, Dordrecht, Boston, London, 299 pp.

Camillo, P. J., Gurney, R. J. and Schmugge, T. J.: 1983, 'A Soil and Atmospheric Boundary Layer Model for Evapotranspiration and Soil Moisture Studies', *Water Res. Research* **19**, 371–380.

Clapp, R. B. and Hornberger, G. M.: 1978, 'Empirical Equations for Some Hydraulic Properties', *Water Res. Research* **14**, pp. 601–604.

De Vries, D. A.: 1963, 'Thermal Properties of Soils', in *Physics of Plant Environment*, Van Wijik, North Holland, Amsterdam, pp. 210–235.

De Vries, D. A.: 1975, 'Heat Transfers in Soil', in D. A. De Vries and N. H. Afgan (eds.), *Heat and Mass Transfers in the Biosphere. Part 1: Transfer Processes in the Plant Environment*, Scripta Book Company, Washington, D.C., pp. 5–28.

Deardorff, J. W.: 1978, 'Efficient Prediction of Ground Surface Temperature and Moisture with Inclusion of a Layer of Vegetation', *J. Geophys. Res.* **20**, 1829–1903.

Dickinson, R. E.: 1984, 'Modeling Evapotranspiration for Three Dimensional Global Climate Models', *Climate Processes and Climate Sensitivity*, *Geophys. Monogr.* **29**, 58–72.

Duynkerke, P. G.: 1992, 'The Roughness Length for Heat and Other Vegetation Parameters for a Surface of Short Grass', *J. App. Meteorol.* **31**, 579–586.

Fuchs, M. and Tanner, C. B.: 1968, 'Calibration and Field Test of Soil Heat Flux Plate' *Soil. Sci. Soc. Amer. Proc.* **32**, 326–328.

Garratt, J. R.: 1978, 'Transfer Characteristics for a Heterogeneous Surface of Large Aerodynamic Roughness', *Quart. J. R. Meteorol. Soc.* **104**, 491–502.

Garratt, J. R. and Hicks, B. B.: 1973, 'Momentum, Heat and Water Vapour Transfer to and from Natural and Artificial Surfaces', *Quart. J. R. Meteorol. Soc.* **99**, 680–687.

Goutorbe, J. P.: 1991, 'A Critical Assessment of the SAMER Network Accuracy', in T. J. Schmugge and J. C. André (eds.), *Land Surface Evaporation. Measurement and Parameterization*, Springer Verlag, pp. 171–182.

Horton, R. and Wierenga, P. J.: 1983, 'Estimating the Soil Heat Flux from Observations of Soil Temperature near the Surface', *Soil Sci. Soc. of America Journal* **47**, 14–20.

Itier, B.: 1982, 'Une Méthode Simplifiée pour la Mesure du Flux de Chaleur Sensible', *J. Rech. Atmos.* **14**(1), 17–34.

Jacquemin, B. and Noilhan, J.: 1990, 'Sensitivity Study and Validation of a Land Surface Parameterization Using the Hapex-Mobilhy Data Set', *Boundary-Layer Meteorol.* **52**, 93–134.

Jackson, R. D., Reginato, R. J., Kimball, B. A. and Nakayama, F. S.: 1974, 'Diurnal Soil Water Evaporation: Comparison of Measured and Calculated Soil Water Fluxes', *Soil Sci. Soc. Amer. Proc.* **38**(6), 861–866.

Kondo, J., Saigusa, N. and Sato, T.: 1990, 'A Parameterization of Evaporation from Bare Soil Surfaces', *J. Appl. Meteorol.* **29**, 385–389.

Laurent, J. P.: 1989, 'Evaluation des Paramètres Thermiques d'un Milieu Poreux: Optimisation d'Outils de Mesure "in situ"', *Int. J. Heat Mass Transfer* **32**(7), 1247–1259.

Mahfouf, J. F.: 1990, 'A Numerical Simulation of the Surface Water Budget During Hapex-Mobilhy', *Boundary-Layer Meteorol.* **53**, 2201–222.

Mahfouf, J. F. and Jacquemin, B.: 1989, 'A Study of Rainfall Interception Using a Land-Surface Parameterization for Mesoscale Meteorological Models', *J. Appl. Meteorol.* **28**, 1282–1302.

Mahfouf, J. F. and Noilhan, J.: 1991, 'Comparative Study of Various Formulations of Evaporation from Bare Soil Using in-situ Data', *J. Appl. Meteorol.* **30**(9), 1354–1365.

Menenti, M.: 1984, 'Physical Aspects and Determination of Evaporation in Deserts Applying Remote Sensing Techniques', Instituut voor Cultuurtechnik en Waterhuishouding, Wageningen, The Netherlands, 202 pp.

Monin, A. S. and Obukhov, A. M.: 1954, 'Basic Laws of Turbulence Mixing in the Ground Layer of the Atmosphere', *Tr. Geofiz. Inst. Aka. Nauk, SSSR*, **24**, 163–187.

Nerry, F.: 1992, Personal communication.

Noilhan, J. and Planton, S.: 1989, 'A Simple Parameterization of Land Surface Processes for Meteorological Models', *Mon. Weather Review*, **117**, 536–549.

Owen, P. R. and Thomson, W. R.: 1963, 'Heat Transfer Across Rough Surfaces', *J. Fluid Mech.* **15**, 321–334.

Passerat de Silans, A.: 1986, 'Transferts de Masse et de Chaleur dans un Sol Stratifié Soumis à Une Excitation Atmosphérique Naturelle. Comparaison Modèle-Expérience', Ph.D. thesis, Institut National Polytechnique de Grenoble, Grenoble, France, 205 pp.

Passerat de Silans, A., Bruckler, L., Thony, J. L. and Vauclin, M.: 1989, 'Numerical Modeling of Coupled Heat and Water Flows during Drying in a Stratified Bare Soil. Comparison with Field Observations', *J. Hydrol.* **105**, 109–138.

Paulson, C. A.: 1970, 'The Mathematical Representation of Wind Speed and Temperature Profiles in the Unstable Atmospheric Surface Layer', *J. Appl. Meteorol.* **9**, 857–861.

Philip, J. R. and De Vries, D. A.: 1957, 'Moisture Movements in Porous Materials under Temperature Gradients', *Trans. Am. Geophys. Union* **38**, 222–232.

Sasamori, T.: 1970, 'A Numerical Study of Atmospberic and Soil Boundary Layers', *J. Atmos. Sci.* **27**, 1123–1137.

Sellers, P. J., Hall, F. G., Asrar, G., Shebel, D. E. and Murphy, R. E.: 1988, 'The First ISLSCP Field Experiment (FIFE)', *Bull. Amer. Meteorol. Soc.* **69**, 22–27.

Sellers, P. J., Mintz, Y., Sud, Y. C. and Dalcher, A.: 1986, 'The Design of a Simple Biosphere Model (Sib) for use within General Circulation Models', *J. Atmos. Sci.* **43**, 505–531.

Van de Griend, A. A., Camillo, P. J. and Gurney, R. J.: 1985, 'Discrimination of Soil Physical Parameters, Thermal Inertia and Soil Moisture from Diurnal Surface Temperature Fluctuations, *Water Res. Research* **21**(7), 997–1009.

Vachaud, G., Vauclin, M. and Colombani, J.: 1981, 'Bilan Hydrique dans le Sud Tunisien. I. Caractérisation Experimentale des Transferts dans la Zone Non Saturée', *J. Hydrol.* **49**, 31–52.

Vauclin, M., Haverkamp, R., Carrillo, E., Gaudet, J. P., Laty, R., Laurent, J. P., Thony, J. L. and Vanderwaare, J. P.: 1992, 'Basic Description of Soil Data Sets and Some Preliminary Results of the EFEDA-Spain Field Campaign', First EEC EFEDA Report, Berlin, January 1992, 26–37.

Wang, J. and Mitsuta, Y.: 1992, 'Evaporation from Desert: Some Preliminary Results of HEIFE', Research Note, *Boundary-Layer Meteorol.* **59**, 413–418.